J. Fluid Mech. (1986), *vol.* 164, *pp.* 107–125
Printed in Great Britain

The stress tensor in a two-dimensional granular shear flow

By CHARLES S. CAMPBELL AND AILING GONG
Department of Mechanical Engineering, University of Southern California, Los Angeles, California 90089–1453

(Received 2 January 1985 and in revised form 6 September 1985)

A computer simulation is used to make a detailed study of the stress tensor in a simple shear flow of two-dimensional disks. The stresses are shown to arise from two momentum-transfer mechanisms: the 'streaming' or kinetic mode, by which momentum is carried by particles as they move through the bulk material; and the collisional mode, by which momentum is transferred from one point to another in the material by interparticle collisions. As might be expected, the results show that the streaming mode dominates at disperse packings and the collisional mode dominates at dense packings. The friction coefficient, the ratio of shear to normal forces, is shown to decrease at high particle packing for both the collisional and streaming modes of transport. Normal-stress differences are observed within the shear plane and are evident in both the streaming and collisional parts.

1. Introduction

The many unexplained problems found in industrial processes that must handle granular materials have prompted a great body of both theoretical and experimental work. As the research continues, the complexity of the physical processes involved are becoming more and more apparent. Most studies have concentrated on two limiting flow regimes. Slow deformations of granular assemblies generally do not flow as individual particles, but as groups of particles yielding along slip lines. Such flows are often described by methods derived from metal-plasticity theory and fall into the 'quasi-static' flow regime. The current state of knowledge has been recently reviewed by Spencer (1981) and Mroz (1980). At the opposite extreme is the 'rapid-flow' or 'grain-inertia' regime, reviewed by Savage (1984). This is best thought of as any flow in which the particle interactions can be described as instantaneous collisions. The present work is directed towards understanding of the latter flow regime.

The pioneering work on the constitutive properties of granular flows was performed by Bagnold (1954). He studied suspensions of wax spheres in a glycerin–water–alcohol mixture sheared in a Couette shear cell and showed that, at even moderate concentrations and shear rates, the composite *ceases* to behave like a Newtonian fluid with a corrected viscosity and adopts the behaviour

$$\tau_{ij}^{*} = \rho_{\mathrm{p}} f_{ij}(\nu) R^2 \left(\frac{\mathrm{d}u}{\mathrm{d}y}\right)^2, \tag{1.1}$$

where τ_{ij}^{*} is the stress tensor, ρ_{p} is the density of the solid material, f_{ij} is a tensor-valued function of the solid fraction ν ($\nu = \rho/\rho_{\mathrm{p}}$ is the fraction of a unit volume that is occupied by solid), R is the particle radius, and $\mathrm{d}u/\mathrm{d}y$ is the local velocity gradient. This rule has been confirmed for dry granular materials by Savage & Sayed (1984),

Hanes (1983), Hanes & Inman 1985), and by the fluid-free computer simulation of Campbell & Brennen (1985*a*). In fact, this behaviour may be anticipated from a simple dimensional analysis. As such, it is not surprising that all theoretical analyses, starting with the heuristic arguments of Bagnold (1954) and continuing through the progressively more sophisticated work of McTigue (1978), Kanatani (1979*a*, *b*, 1980), Ackermann & Shen (1979), Ogawa & Oshima (1977), and Oshima (1978, 1980), have shown similar behaviour. The most comprehensive studies along these lines, described in Savage & Jeffrey (1981), Jenkins & Savage (1983), Lun *et al.* (1984) and Lun & Savage (1985), are derived from Enskog's dense-gas model (see Chapman & Cowling 1970). However, the work of Campbell & Brennen (1985*a*, *b*) indicates that simple shear flows may represent an anomalously simple case of granular flow and that (1.1) may not be universally valid. A similar conclusion can be drawn from Jenkins & Savage (1983), Lun *et al.* (1984) and Lun & Savage (1985), although no demonstration is presented.

The primary obstacle to understanding granular flows is the almost total lack of adequate experimental techniques and instrumentation. For example, the Couette-shear-cell experiments, that constitute the only experimental support of (1.1), only report measurements of two of the nine components of the stress tensor: τ^*_{xy}, the shear stress and τ^*_{yy}, the normal stress, on the cell walls. No measurements have been made of the other stress-tensor components, although Savage (1979) has presented a heuristic demonstration of stress generation normal to the shear plane.

While the bulk mechanics of a granular material are a slowly unfolding mystery, the mechanisms of particle interaction: collisions, surface friction, elastic deformation, etc. are all well established. Around these basic interactions, computer simulations can be build that follow the individual trajectories of the constituent particles and accurately describe the behaviour of the bulk material. Such simulations have been constructed by Campbell (1982), Campbell & Brennen (1985*a*, *b*), Walton (1980, 1982*a*, *b*) and Cundall (1974), and have proven to be useful investigative tools for granular-material flows. In a computer simulation, everything is known about the simulated system so that any information can be found by statistical averaging. The purpose of the present investigation is to use a computer simulation to make a detailed study of the stress tensor in a Couette flow of granular material.

2. Computer simulation

The simulation used here differs only slightly from that described fully in Campbell (1982) and to a lesser extent in Campbell & Brennen (1985*a*, *b*), and so will be even more briefly described here.

Throughout the simulation, the particles (of mass m and radius R) are confined within a control volume such as that shown schematically in figure 1. To simulate a Couette flow, both the top and bottom of the control volume are closed by solid boundaries. The solid walls are separated by a distance H and the upper wall is given a velocity U in the x-direction relative to the bottom wall. The sides of the control volume are bounded by 'periodic' boundaries; as a particle passes through one periodic boundary it re-enters the other with exactly the same position and relative velocity with which it left. This type of boundary gets its name because it emulates a situation in which the entire control volume is periodically repeated infinitely many times upstream and downstream. This setup greatly enhances the computational efficiency of the simulation by limiting the number of particles to those initially placed

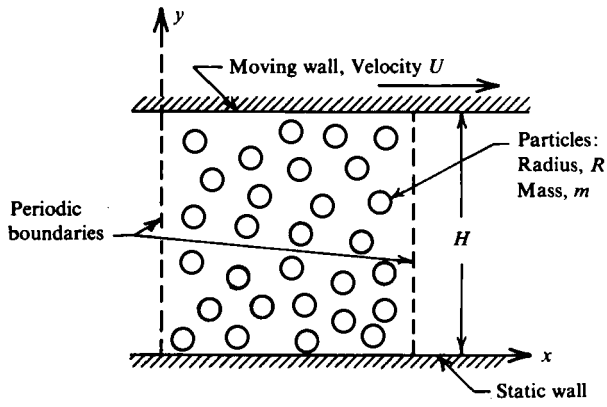

FIGURE 1. Schematic of the Couette-flow simulation.

in the control volume. (All of the current work was performed on control volumes of eighty particles.) It has the drawback that it is only applicable to flows with no gradients in the flow direction (i.e. steady, unidirectional flows).

After the initial conditions are set, the simulation is allowed to proceed until it converges to a steady state. Attainment of a converged state must be determined from some instantaneously observable parameters. For these Couette-flow simulations, a converged state was assumed to occur when the total system kinetic energy and the solid-wall spacing H achieve nearly constant values. The determination of convergence is hindered because both parameters fluctuate slightly. For most of the calculations, convergence was achieved after as little as 500 collisions per particle from the initial state. After convergence is obtained, properties are averaged over long periods of time (up to 3000 collisions per particle).

Each particle collision is assumed to occur instantaneously once the particle surfaces come into contact. (This is essentially the hard-sphere approximation often used in the kinetic theory of gases.) The collision result is computed from a standard centre-of-mass collision solution. Because the particles rotate as well as translate, two conditions are required to close the system of equations: one for the relative particle velocities normal to the particle surfaces at contact and the other for the particle velocities tangential to the surface at the contact point. The normal-velocity condition assumes that the particles are nearly elastic in the sense that energy is dissipated as a result of the collision but the particles involved do not deform. This is realized through a coefficient of restitution e ($e < 1$), which is the ratio of the approach-to-recoil velocities and is specified as an input parameter to the program. The tangential-velocity condition assumes that, on departure after a collision, there will be zero relative tangential velocity between the surface of the particles. This will be called a 'fully rough' surface condition, as it corresponds to an infinite surface-friction angle. (It should not be confused with the artificial rough-surface conditions used in kinetic-theory models of gases which do not dissipate energy. In this case, both the normal and tangential conditions result in energy dissipation.) On collision with a solid boundary, a particle recoils with the same relative speed with which it approached, and, at the same time, assumes the same tangential velocity as the wall with no change to its rotational speed. This is essentially the same as the 'type B' wall boundary condition that was reported in Campbell & Brennen (1985*a*). It is used

here because it resulted in uniform velocity-gradient and density profiles and thus creates an ideal environment from which to study flow properties such as the stress tensor.

3. The granular stress tensor

The continuum stresses are a byproduct of the microscale mechanisms of momentum transfer within the material. For granular materials and hard-sphere models of gases, momentum is transferred in two modes. The 'streaming' or 'kinetic' mode describes the transport of momentum as a particle moves through the material carrying its momentum with it. The 'collisional' mode, as the name implies, describes the transport of momentum by interparticle collisions. In a collision momentum is exchanged between the two particles. The magnitude of the momentum exchange is the impulse associated with the collision which is carried a distance corresponding to the sum of the two particle radii in the direction of the line connecting their centres. Both mechanisms make important contributions to the stress tensor in a granular flow. Obviously, the streaming mode will dominate at low densities where collisions are infrequent and the collisional mode will be dominant at high densities as the particles cannot move far between collisions.

The complete stress tensor is determined by summing the measured values for both the collisional and streaming contributions, each of which is determined in a manner to be described in §§3.1 and 3.2. The results are shown in figure 2. The numerical values are verified by comparing the τ^*_{xy} and τ^*_{yy} components with the stresses exerted on the solid walls. The measured values for the off-diagonal stress-tensor components were found to be equal to within three significant digits. Thus no graph is plotted for the τ_{yx} component. As for all that are to follow, these results are scaled as:

$$\tau_{ij} = \frac{\tau^*_{ij}}{\rho_p R^2 (U/H)^2}, \tag{3.1}$$

where τ^*_{ij} is the original unscaled result. A simple dimensional analysis indicates that the resulting dimensionless stresses should be functions only of the particle coefficient of restitution ϵ and some dimensionless measure of the particle packing, here represented as the solid fraction ν. (For this flow geometry and boundary conditions, the scaled value τ_{ij} is interchangeable with f_{ij} in (1.1).) Note that the normal stresses τ_{xx} and τ_{yy} are plotted as absolute values; except where noted, all of the normal stresses are negative (compressive stresses) and the shear stresses are positive.

Also plotted are the predictions of Lun *et al.* (1984). As their results were derived for spherical particles instead of the cylindrical particles used in the simulation, the solid fraction is subject to different interpretation. (For the two-dimensional case, ν is, in effect, a ratio of areas instead of a ratio of volumes.) In particular, the maximum values of the solid fraction for which the material can be sheared are different in the two cases. To make an appropriate comparison, here, as in Campbell & Brennen (1985*a*), an equivalent solid fraction is defined based on similar average particle spacing:

$$\nu = (\tfrac{2}{3}\pi^{\frac{1}{2}}\nu^*)^{\frac{2}{3}}, \tag{3.2}$$

where ν^* is the spherical-particle solid fraction (The results of the computer simulation for the stresses exerted on the sidewalls were shown by Campbell & Brennen (1985*a*) to agree well with experimental results when the density was scaled

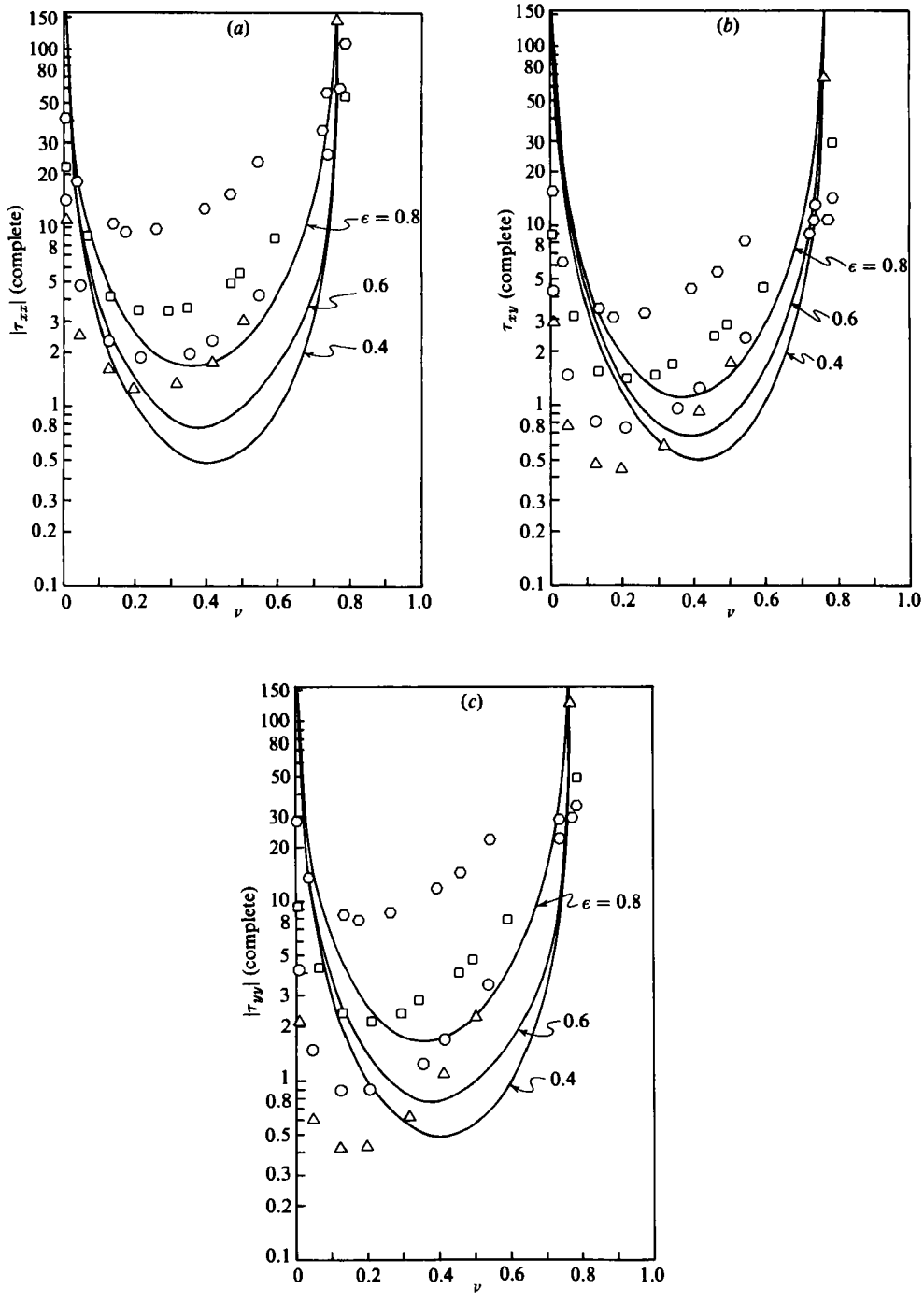

FIGURE 2. The complete dimensionless stress tensor as a function of the solid fraction ν: (*a*) τ_{xx}; (*b*) τ_{xy}; and (*c*) τ_{yy}. The lines are derived from Lun *et al.* (1984). △, $\epsilon = 0.4$; ○, 0.6; □, 0.8; ⬡, $\epsilon = 1.0$.

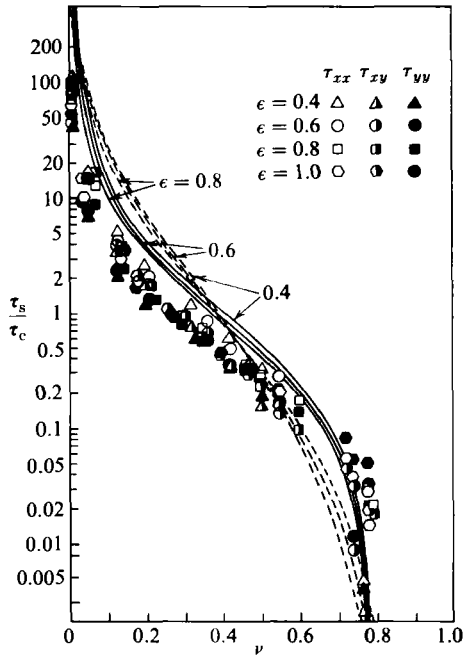

FIGURE 3. The ratio τ_s/τ_c of streaming to collisional contributions to the stress tensor as a function of the solid fraction ν. The lines are derived from Lun *et al.* (1984), ——, τ_{xx}, τ_{yy}; – – –, τ_{xy}.

in this manner.) Also, on the suggestion of Savage (1984, personal communication), the pair distribution function used by Lun *et al.* (1984) has been replaced by

$$g(\nu^*) = \frac{1}{(1-(\nu^*/\nu_m^*))^{\frac{5}{2}\nu^*}}, \tag{3.3}$$

where ν_m^* is the maximum shearable solid fraction, here taken to be $\nu_m^* = 0.52$ ($\nu_m = 0.78$), at which point the particles are arranged in a square array. This is shown in Campbell & Brennen (1985*a*) to be the effective upper limit on the solid fraction that can still undergo a shearing motion. (Lun *et al.* originally used the pair distribution function found in Carnahan & Starling (1969) which predicted the necessary asymptotic behaviour at $\nu = 1.0$ instead of the lower, more realistic, values allowed by (3.3).) No theoretical line is shown for $\epsilon = 1.0$ as there would then be no dissipation mechanism in the Lun *et al.* theory to damp the random motions. (In the simulation, the fully rough particle surfaces always provide a dissipation mechanism.)

Considering the difficulty of making such a comparison, there is remarkably good agreement between the measured and theoretical stresses. Each appears to asymptote to infinity both as $\nu \to 0$ and as the solid fraction approaches its maximum shearable limit at about $\nu_m = 0.78$. The reason for the high-density asymptote is clear; beyond the shearable limit, infinite forces would be required to shear the material. The reason for the low-density asymptote is less apparent. Here the authors accept the reasoning of Lun *et al.* (1984) that, at such low densities, interparticle collisions are infrequent and the random particle velocities are not damped by the collisional inelasticity. This results in large random velocities and correspondingly large streaming contributions to the stress tensor.

This low-density asymptote is imposed by the streaming contribution and the

high-density asymptote is imposed by the collisional contribution. The importance of each contribution is shown in figure 3. The ratio τ_s/τ_c, where τ_s and τ_c respectively represent the streaming and collisional stress-tensor contributions, varies over four orders of magnitude within the range of solid fractions studied. Moreover, the ratio appears to depend only on solid fraction; no variation with ϵ or the stress-tensor component can be ascertained from the data. The theoretical lines from Lun *et al.* (1984) are also plotted and predict a slight variation with ϵ and the stress-tensor component. However, such variations are so small that they could easily lie within the data scatter.

3.1. *The streaming stress tensor*

The streaming portion of the stress tensor τ_s is a byproduct of the random, almost thermal, motion of the granules. By virtue of its motion, each particle transports its own momentum as it moves through the bulk material. From arguments presented in, for example, Chapman & Cowling (1970), the resulting contribution to the stress tensor is

$$\tau_s^* = \rho_p \nu \begin{pmatrix} \langle u'^2 \rangle & \langle u'v' \rangle \\ \langle u'v' \rangle & \langle v'^2 \rangle \end{pmatrix}, \tag{3.4}$$

where the primed quantities indicate the instantaneous deviation from the appropriate mean-velocity component. The $\langle\ \rangle$ represents the average of the appropriate system properties, sampled at regular intervals, over a long period of system time – about 2500 collisions per particle. (For more details about the averaging process, the reader is referred to Campbell 1982.) Each term of the stress tensor is determined by the formula

$$\langle p'q' \rangle = \langle pq \rangle - \langle p \rangle \langle q \rangle \tag{3.5}$$

in exactly the same way as the Reynolds stresses.

The similarity of (3.4) to the Reynolds-stress tensor is no accident. Both reflect the momentum flux due to random motion of the respective materials. The major differences are the physical motivation that lead to the random movement and a technical one, that $\langle\ \rangle$ represents an average over discrete samples. In a granular material, the random motion is an unavoidable byproduct of interparticle collisions. The strength of the random motion generated during a collision will be proportional to the relative velocity of the particles before collision which, in an averaged sense, will be related to the shear rate (U/H) within the bulk material. As energy associated with the random motion is dissipated by subsequent collisions, a continuous flux of energy down from the main shear flow is required to maintain the random velocities. Thus the magnitude of the random particle velocity should be related in some way to the shear rate. To illustrate this, it is convenient to define a parameter S:

$$S = \frac{2RU}{HT^{\frac{1}{2}}}, \tag{3.6}$$

where $T = \langle u'^2 \rangle + \langle v'^2 \rangle + \beta R^2 \langle w'^2 \rangle$ is a measure of the magnitude of the energy associated with random particle velocities. (Making an analogy with the thermal motion of molecules, T is often referred to as the 'granular temperature'.) S is plotted as a function of ν in figure 4. Also plotted are the corresponding curves predicted by Lun *et al.* (1984). This comparison is somewhat questionable as the curve predicted by Lun *et al.* was derived for smooth spherical particles and compared with data from a simulation of rough cylindrical particles. In going from spherical to cylindrical particles, a component of temperature, associated with the out-of-shear-plane motion,

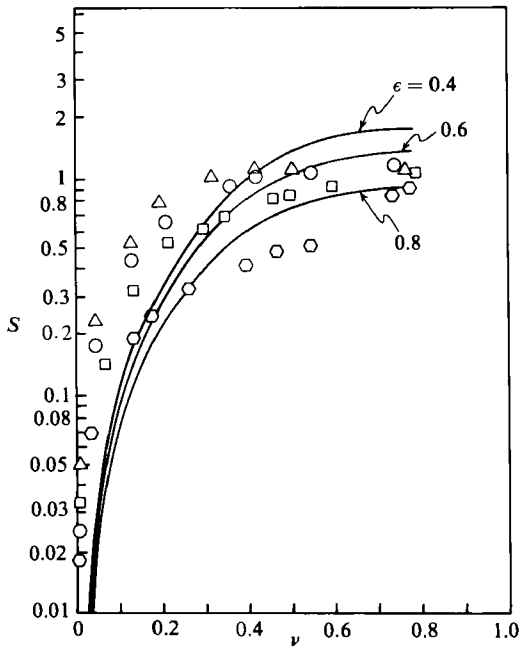

FIGURE 4. The dimensionless parameter S (equation (3.1.3)) as a function of the solid fraction ν. The lines are derived from Lun *et al.* (1984). Symbols as in figure 2.

is lost, but, at the same time, the rough particle surfaces add a temperature component due to the random rotational motion. Thus the comparison with Lun *et al.* is only strictly valid if there is equipartition of energy between the out-of-plane translation and the rotational modes. The validity is affirmed only by the relatively close agreement between the prediction and the simulation results.

Figure 5 shows the streaming contribution to the stress tensor. As expected, it is large for small values of the solid fraction, first decreasing rapidly and then levelling off with ν. This is in accord with the predictions of Lun *et al.* (1984). But then a curious thing happens. As the shearable packing limit is approached, the τ_{xy} component again drops rapidly. Similar behaviour is observed in the normal stress components, but only for the $\epsilon = 1.0$ measurements. For smaller values of ν the τ_{xx} component remains roughly constant, as predicted by Lun *et al.*, while the τ_{yy} components rise gently. No physical explanation for this phenomenon is immediately apparent; however, it is a moot problem, as it occurs only in the region where the collisional contribution is dominant.

3.2. *The collisional stress tensor*

At high densities, the majority of the momentum transfer will be accomplished through interparticle collisions. A diagram of the collision analysis is shown in figure 6. Each collision imparts an impulse, the strength of which depends on the relative motion of the particles before collision. The impulse exerted at collision is

$$\boldsymbol{J} = m\left(\tfrac{1}{2}(1+\epsilon)\,(\boldsymbol{q}\cdot\boldsymbol{k})\,\boldsymbol{k} + \frac{1}{2(1+1/\beta)}\,(\boldsymbol{q}-(\boldsymbol{q}\cdot\boldsymbol{k})\,\boldsymbol{k} + R(\boldsymbol{\omega}_1+\boldsymbol{\omega}_2)\times\boldsymbol{k})\right), \tag{3.7}$$

where $\boldsymbol{q} = \boldsymbol{u}_1 - \boldsymbol{u}_2$ is the relative velocity of the particles just before collision, $\boldsymbol{\omega}_1$ and $\boldsymbol{\omega}_2$ their respective rotation rates (for 2-D flows, $\boldsymbol{\omega}_1$ and $\boldsymbol{\omega}_2$ are always oriented

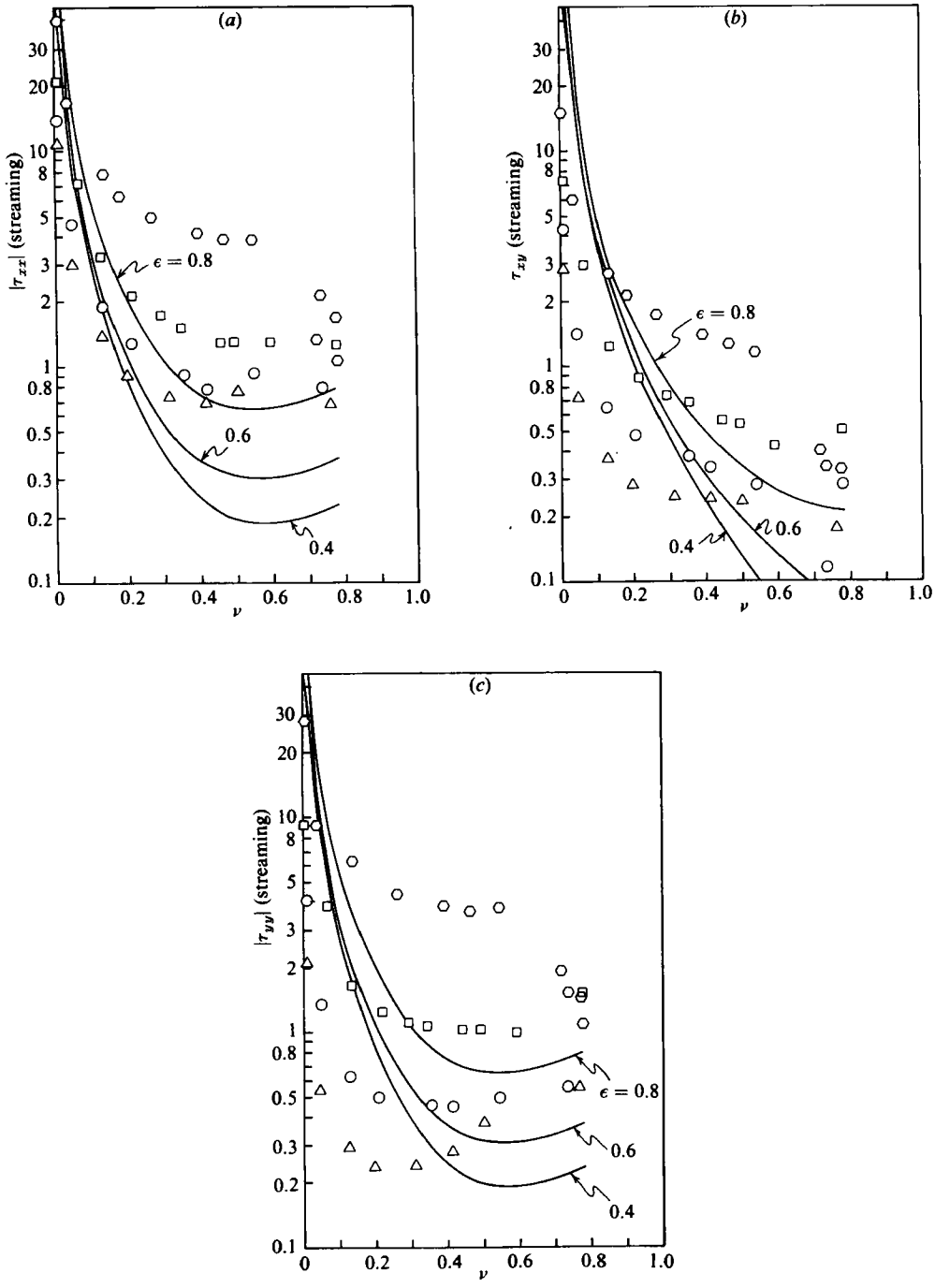

FIGURE 5. The streaming contribution to the stress tensor as a function of the solid fraction: (*a*) τ_{sxx}; (*b*) τ_{sxy}; (*c*) τ_{syy}. The lines are derived from Lun *et al.* (1984). Symbols as in figure 2.

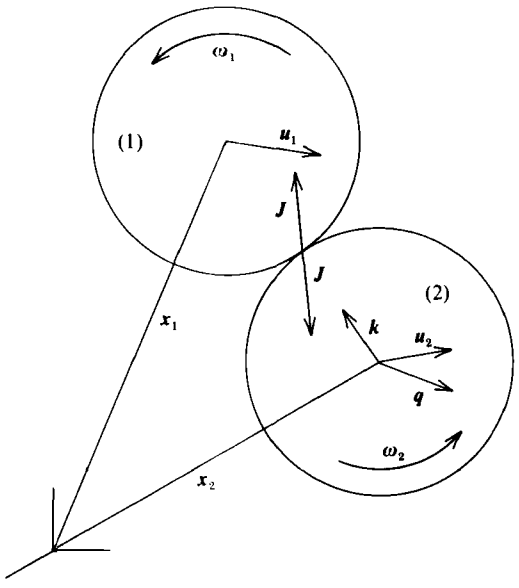

FIGURE 6. Diagram for the collision analysis.

perpendicular to the shear plane), $\boldsymbol{k} = (\boldsymbol{x}_1 - \boldsymbol{x}_2)/\| \boldsymbol{x}_1 - \boldsymbol{x}_2 \|$ is the unit vector pointing along the line connecting the particle centres directly at collision, and β is the square of the ratio of the particle radius of gyration to the particle radius ($\beta = 0.5$, the value appropriate for cylinders, is used throughout this work).

As the collisions are instantaneous, each collision results in an instantaneous momentum exchange of strength J between the two particles. From a transport point of view, the effect of a collision is the transport of J momentum a distance $2R$ in the direction $\boldsymbol{k}$. The effective force exerted by the collision, on a surface separating the particles, is $2RJ\boldsymbol{k}\cdot\boldsymbol{n}$, where $\boldsymbol{n}$ is the vector normal to the surface. The portion of the stress tensor $\boldsymbol{\tau}_c$ that is due to interparticle collisions is thus given by

$$\boldsymbol{\tau}_c = 2R[J\boldsymbol{k}], \tag{3.8}$$

where $[J\boldsymbol{k}]$ is found by summing the dyadic product $J\boldsymbol{k}$ for every collision and then normalizing the result by dividing by the system volume and the length of the averaging period. (Physically the [ ] average should be interpreted in the same way as the $\langle\ \rangle$ average multiplied by the collision rate.)

The collisional contribution to the stress tensor is plotted in figure 7 as a function of the solid fraction ν. There is nothing surprising here. The measurements increase steadily with solid fraction and diverge asymptotically near the shearable limit. Compared with the streaming measurements, the values appear to make up the high-density half of the complete stress-tensor curves. Also shown are the predictions of Lun *et al.* (1984) for smooth spheres and the more recent work of Lun & Savage (1985) who analysed the collisional stress tensor for rough spheres. It should be noted in comparing these two theories that Lun & Savage's is derived from the earlier and less exact calculations of Jenkins & Savage (1983) rather than the more exact treatment used in Lun *et al.* (1984) and, furthermore, takes no account of the streaming contribution to the stress tensor.

The collision impulse given in (3.7) may be divided into three parts: that due to the relative motion of the particles normal to the particle surface at the contact point;

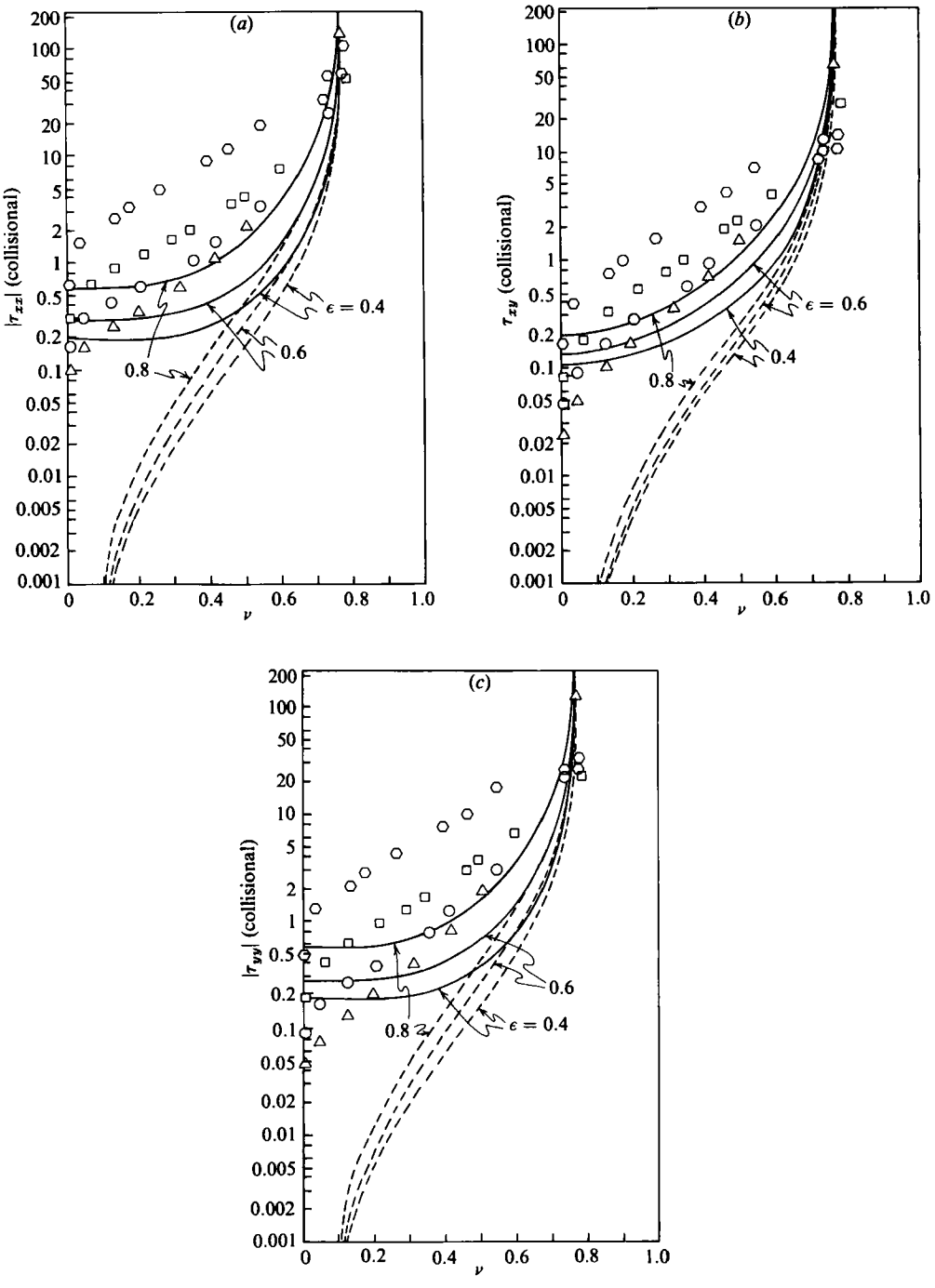

FIGURE 7. The collisional contribution to the stress tensor as a function of the solid fraction ν: (*a*) τ_{cxx}, (*b*) τ_{cxy}, (*c*) τ_{cyy}. ——, Lun *et al.* (1984); – – –, Lun & Savage (1985); symbols as in figure 2.

that tangential to the surface at the contact point; and the particle rotations. Each part of the impulse makes its own contribution to the collisional stress tensor. That due to the normal component of velocity at collision is

$$\boldsymbol{\tau}_{\mathrm{N}}^{*} = mR(1+e)[(\boldsymbol{q}\cdot\boldsymbol{k})\boldsymbol{kk}], \tag{3.9}$$

that due to the relative velocity tangential to the surfaces at the contact point is

$$\boldsymbol{\tau}_{\mathrm{T}}^{*} = \frac{mR}{1+1/\beta}[(\boldsymbol{q}-(\boldsymbol{q}\cdot\boldsymbol{k})\boldsymbol{k})\boldsymbol{k}] \tag{3.10}$$

and that due to the particle rotations is

$$\boldsymbol{\tau}_{\omega}^{*} = \frac{mR^2}{1+1/\beta}[(\boldsymbol{\omega}_1+\boldsymbol{\omega}_2)\times\boldsymbol{kk}]. \tag{3.11}$$

The three constituents of the collisional stress tensor are plotted in figure 8 as functions of the solid fraction ν. (Note that, in this plot, the signs of the components are explicitly stated in the legend as the constituents may make contributions of differing sign to each component.) The major contribution to the collisional stress tensor comes from $\boldsymbol{\tau}_{\mathrm{N}}^{*}$. Except for extremely low densities, the tangential and rotational contributions have almost the same magnitude, which is at least an order of magnitude smaller than the normal contribution. Note also that, while the magnitudes of the rotational and tangential contributions are identical in the normal stresses τ_{xx} and τ_{yy}, the signs of the contributions have changed. That is, the tangential portion of the collisional stress tensor contributes a compressive stress to τ_{xx} and a tensile stress to τ_{yy}. The opposite is true for the rotational portion.

Note that individually the tangential and rotational components, as described by (3.10) and (3.11), are proportional to dyadic products of perpendicular vectors and must necessarily make asymmetric contributions to the stress tensor. In a continuum, the stress tensor must be symmetric in order to assure rotational equilibrium of material elements. However, in a granular flow, the granules can and do have a rotational velocity and the appearance of asymmetry in the stress tensor works to change the average rotational state of the particles. After steady conditions have been reached, there cannot, on the average, be unbalanced torques on the particles. Thus, in the converged state, the stress tensor must be symmetric. This is the case observed in the simulation. Note that the rotational stress tensor depends on the sum of the rotational velocities $\boldsymbol{\omega}_1$ and $\boldsymbol{\omega}_2$ and not on their difference. Thus the mean rotational speed of the particles will accelerate until the asymmetric contribution from the rotational stress tensor cancels the asymmetric contribution from the tangential stress tensor (which in the average sense is dependent on the shear rate U/H), and produces a symmetric result. This can be seen by comparing the τ_{xy} and τ_{yx} plots of figure 8. Note that the sign of the rotational contribution has changed and that the magnitude of the tangential component is significantly smaller in the τ_{yx} plot than in the τ_{xy} plot.

In order to symmetrize the stress tensor, the average rotational speed of the particles converges to a well-defined value that is constant across the flow. This is plotted in figure 9 as a function of the solid fraction ν. As would be expected from both dimensional and physical reasoning, the rotation rate is proportional to the shear rate U/H and, over much of the range of solid fraction, $\langle\omega\rangle = -0.5(U/H)$. Towards the shearable limit, however, $|\omega H/U|$ decreases rapidly. Campbell & Brennen (1985*a*) show that a distinct layered microstructure develops in the flow as this limit is

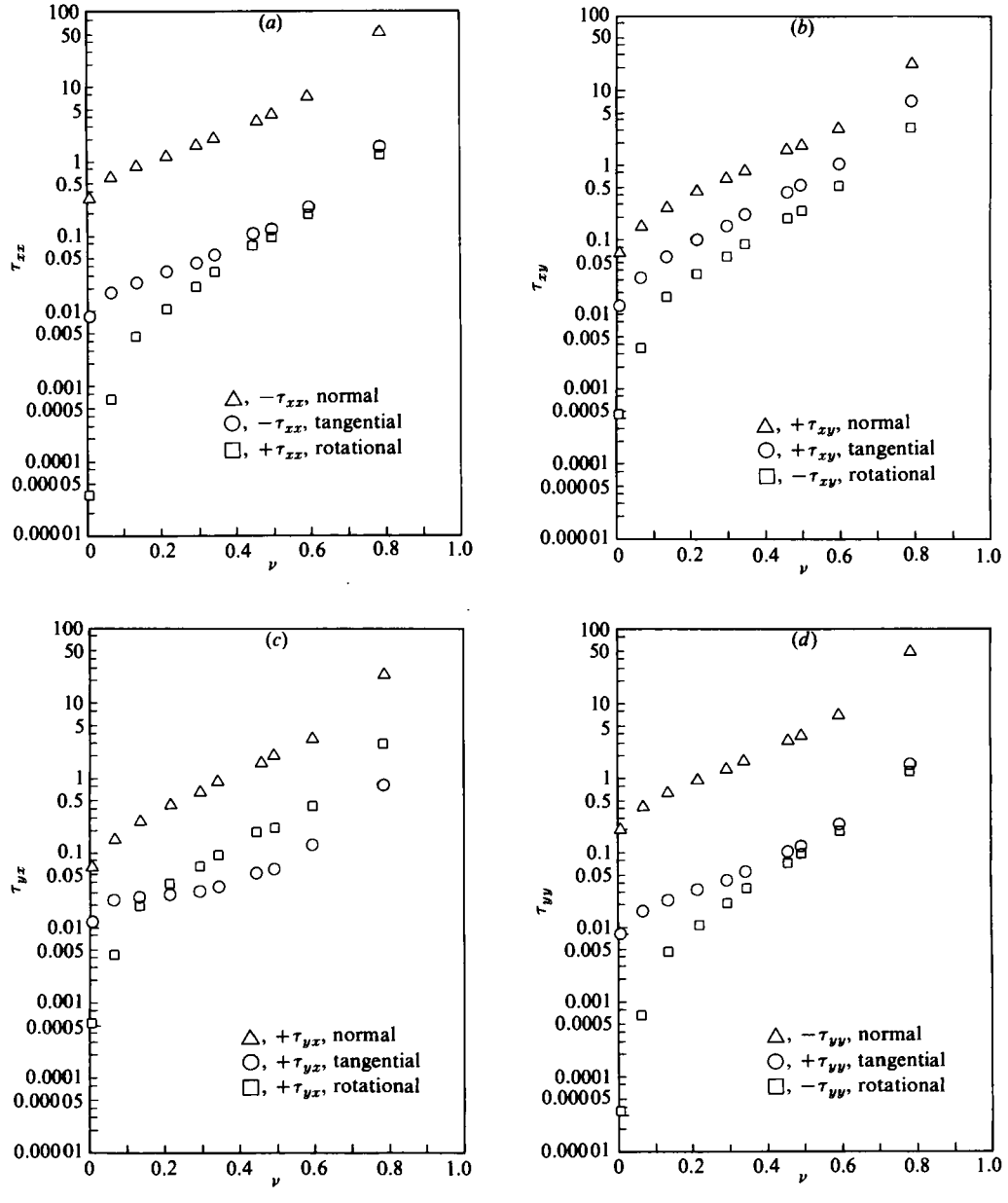

FIGURE 8. The normal, tangential and rotational constituents of the collisional stress tensor as functions of the solid fraction ν: (*a*) τ_{xx}, (*b*) τ_{xy}, (*c*) τ_{yx}, (*d*) τ_{yy}; $\epsilon = 0.8$.

approached; in order to maintain the shear flow, the material is forced to form itself into layers parallel to the flow direction, each layer of particles moving with the appropriate velocity corresponding to its position in the shear flow. The layering limits the angles at which collisions between particles can occur. Some preliminary unpublished calculations along the lines of Savage & Jeffrey (1981) indicate that this observed reduction in $|\omega H/U|$ is one byproduct of the microstructure formation. Notice that no points are plotted for $\nu < 0.1$. At very small ν, the rotation does not

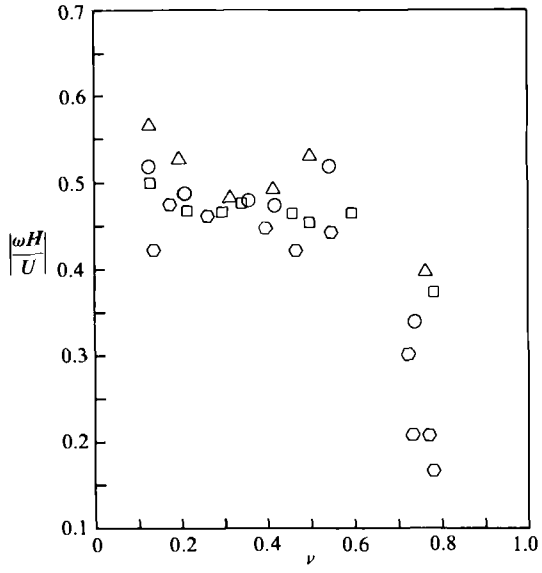

FIGURE 9. The scaled average rotation rate $\omega H/U$, as a function of the solid fraction ν. Symbols as in figure 2.

converge to any constant value. This is not surprising as the rotational control described above is a byproduct of particle collisions, which would be infrequent at such small solid fractions. Furthermore, it explains why the rotational contribution to the collisional stress tensor, as shown in figure 8, becomes insignificant for small solid fractions.

3.3. *The friction coefficient and normal-stress differences*

A standard soil-mechanics test is to shear a static soil sample and to measure the friction coefficient, or ratio of shear-to-normal forces τ_{xy}/τ_{yy} at which the sample yields. The results show that the friction coefficient increases the more densely the sample is initially packed. Savage & Sayed's (1984) experimental studies of fully developed granular flows show exactly the opposite to be true; the friction coefficient was seen to decrease with increasing solid fraction. Similar observations were made in the computer simulation of Campbell & Brennen (1985*a*) and were attributed to anisotropies in the collision-angle distribution induced by the formation of the layered microstructure. The results of the present study, shown in figure 10, indicate that this is only part of the story.

The friction coefficient for the complete stress tensor is plotted in figure 10(*c*) and shows the decrease in friction coefficient with solid fraction that was described above. The effect is much more pronounced for the lower coefficients of restitution than for the larger. In fact, the points corresponding to $e = 0.8$ and $e = 1.0$ appear to be constant over much of the range of solid fraction. Along with the data points are plotted the predictions of Lun *et al.* (1984). As the rough particle surfaces could significantly affect the behaviour of the friction coefficient, also plotted is the corresponding curve derived from a miscegenative hybrid formed by mating the streaming stress tensor of Lun *et al.* (1984) and the rough-particle collisional stress tensor of Lun & Savage (1985). Both theoretical curves deviate strongly from the measurements toward the larger solid fractions.

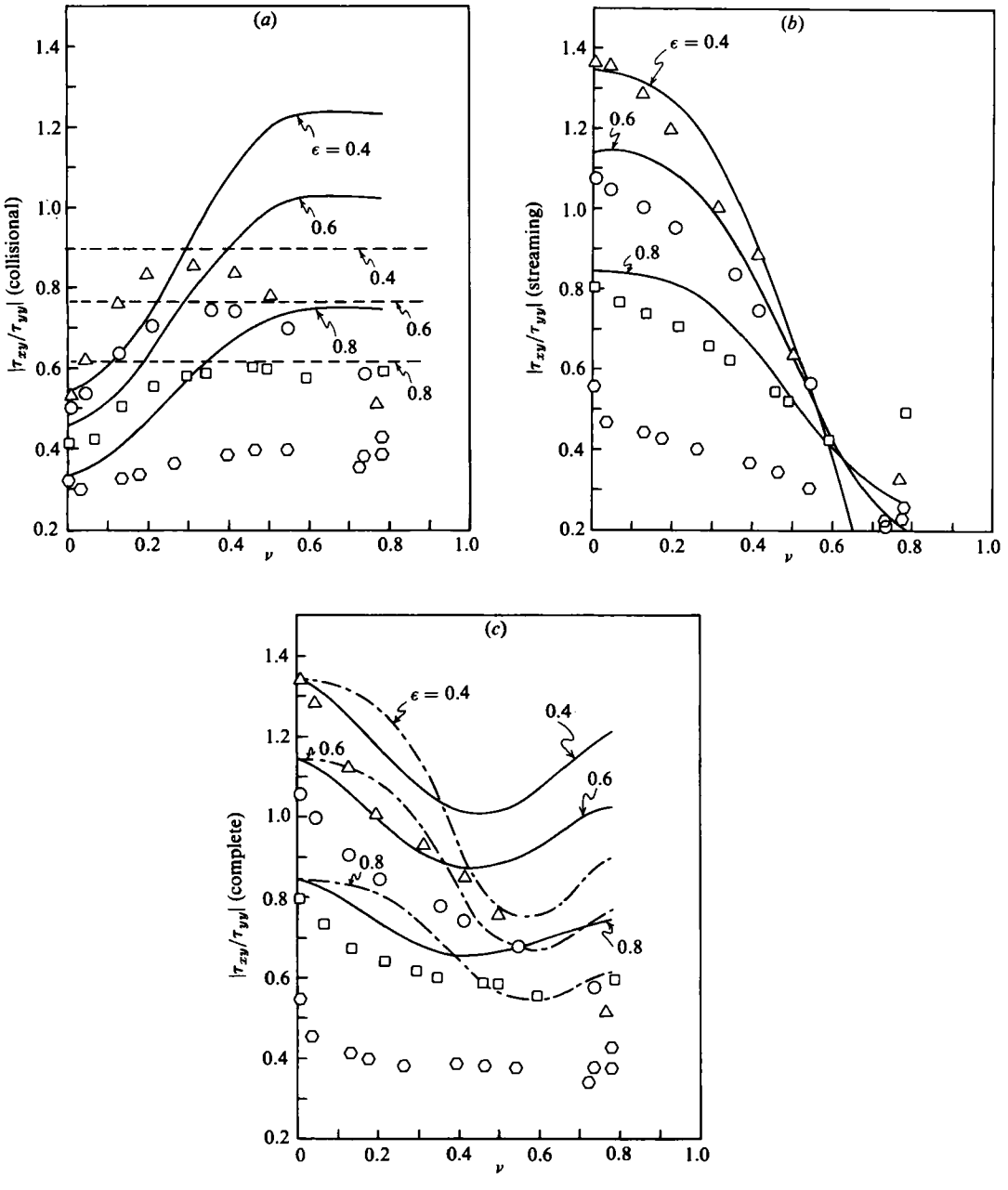

FIGURE 10. The friction coefficient τ_{xy}/τ_{yy} as a function of the solid fraction ν: (*a*) collisional contribution, (*b*) streaming contribution and (*c*) complete stresses; ----, Lun & Savage (1985) hybrid. Other symbols as in figure 7.

Figures 10(*a*) and (*b*) break up the friction coefficient into its collisional and streaming parts. Surprisingly, the major reduction in friction coefficient is found in the streaming and not in the collisional contribution to the stress tensor and thus cannot be directly attributed to the microstructure formation. The behaviour of the streaming component is very accurately predicted by Lun *et al.* (1984). The collisional

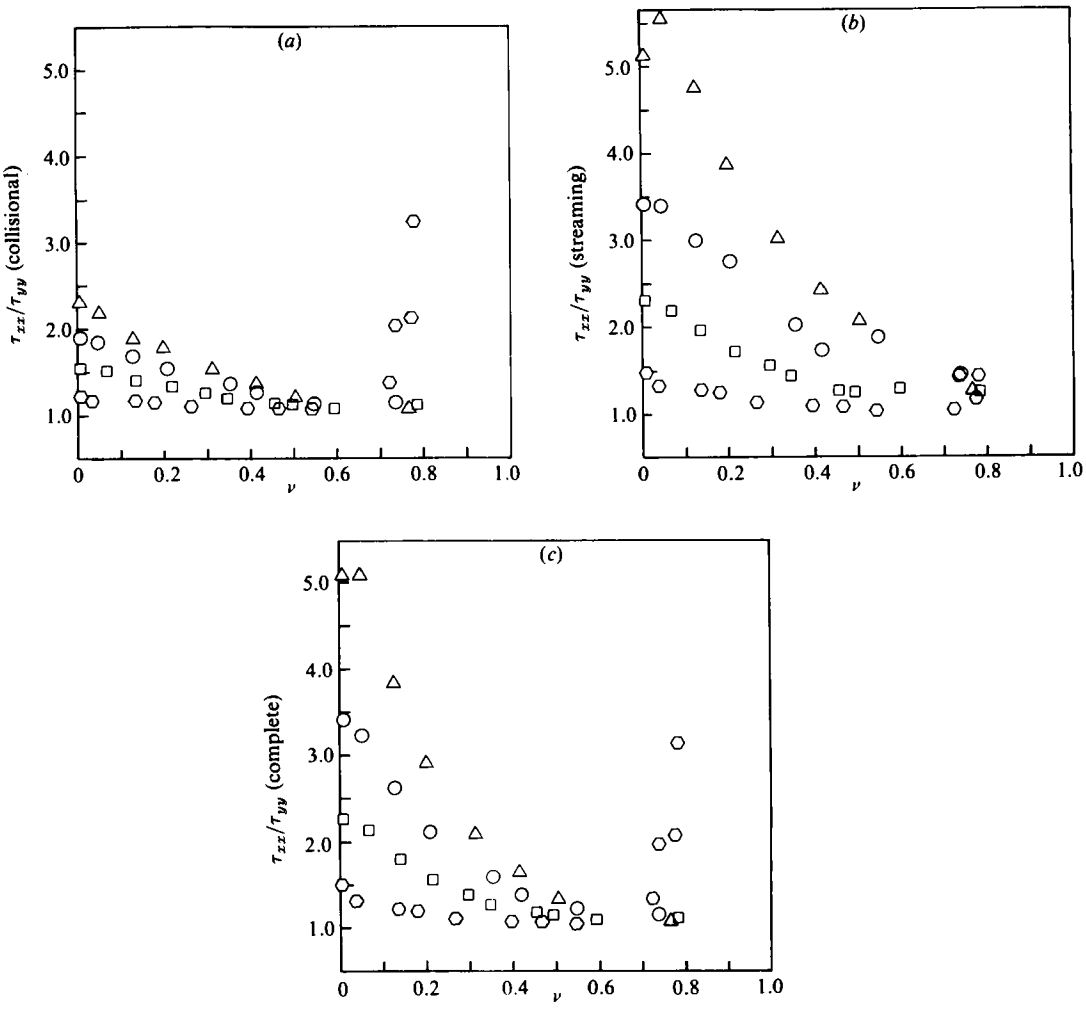

FIGURE 11. The ratio of the normal stresses τ_{xx}/τ_{yy} as function of the solid fraction ν: (*a*) collisional contribution, (*b*) streaming contribution, and (*c*) complete stresses. Symbols as in figure 2.

friction coefficient actually rises for small values of the solid fraction exactly as predicted by Lun *et al.* However, the collisional friction coefficient for the larger coefficients of restitution level off to a constant value, while the smaller decrease as the shearable limit is approached. This behaviour can be attributed to the development of the layered microstructure. The deviation from the Lun *et al.* curves is to be anticipated here as that theory makes no provision for the microstructure development.

All of the theories described so far (Savage & Jeffrey 1981; Jenkins & Savage 1983; Lun *et al.* 1984; and Lun & Savage 1985) predict that the in-the-shear-plane normal stresses τ_{xx} and τ_{yy} should be identical while the out-of-shear-plane normal stress τ_{zz} is somewhat smaller (τ_{zz} is, of course, irrelevant to the present two-dimensional study). The current results, plotted in figure 11, show that τ_{xx} can be significantly greater (by up to a factor of 5) than τ_{yy}, especially for smaller solid fractions and

coefficients of restitution. As the shearable limit is approached, the differences almost, but not entirely, disappear. The major contributor is once again the streaming stress tensor, but the effect of the collisional contribution is not insignificant. (Anomalous behaviour is found at dense packings in the $\epsilon = 1.0$ results, for which the ratio τ_{xx}/τ_{yy} is observed to increase dramatically near the shearable limit.) Some understanding of this effect can be found in figure 8. As noted previously, the tangential and rotational contributions makes contributions of equal magnitude but opposite sign to τ_{xx} and τ_{yy}. But as the magnitude of the tangential contribution is larger in both, the combination increases the magnitude of τ_{xx} relative to τ_{yy}.

4. Conclusions

The stress tensor in a two-dimensional granular shear flow has been investigated using a computer simulation. Two mechanisms of momentum transfer combine to make up the complete stress tensor. The streaming mode, by which momentum is carried by the random motion of particles through the bulk material is dominant for loosely packed materials. The collisional mode, whereby momentum is transferred by interparticle collisions, becomes dominant as the material becomes densely packed. The dimensionless stress given by (3.1) is seen to asymptote to infinity both as ν approaches the shearable limit (a result of the collisional mode) and as ν goes to zero (a result of the streaming mode). This behaviour is in accord with the predictions of Lun *et al.* (1984). The collisional stress tensor is broken up to reveal the individual effect of the normal relative velocity of the particles at collision, the tangential relative velocity of the particles at collision and the rotation of the particles. The normal contribution is by far the most important conveyer of momentum. However, the tangential and rotational contributions individually produce asymmetric stress tensors, but combine to yield a symmetric result. This is accomplished by fixing the mean rotational speed of the particles to a value of about one half the mean-shear rate throughout most of the range of solid fraction. The material friction coefficient is a decreasing function of the solid fraction. This behaviour is shown to be a combined effect of the streaming and collisional modes. Finally, normal-stress differences are observed, an effect that decreases toward the shearable solid-fraction limit.

Professor Richard Kaplan was instrumental in providing the computer facilities used to carry out this investigation. Without his assistance, the quality of these results would have been severely hampered. The authors are most grateful for the support provided by the USC Faculty Research and Innovation Fund and the National Science Foundation under the Presidential Young Investigator Award program, grant number MEA-8352513. Special thanks to Dr George Lea and Professor Christopher Brennen.

REFERENCES

ACKERMANN, N. L. & SHEN, H. 1979 Stresses in rapidly sheared fluid–solid mixtures. *J. Engng Mech. Div. ASCE*, **108**, 95–113.

BAGNOLD, R. A. 1954 Experiments on a gravity-free dispersion of large solid particles in a Newtonian fluid under shear. *Proc. R. Soc. Lond.* A **225**, 49–63.

CAMPBELL, C. S. 1982 Shear Flows of Granular Materials. Ph.D. thesis and *Rep.* E-200.7, Division of Engineering and Applied Science, California Institute of Technology, Pasadena, Ca.

CAMPBELL, C. S. & BRENNEN, C. E. 1985*a* Computer simulation of granular shear flows. *J. Fluid Mech.* **151**, 167–188.

CAMPBELL, C. S. & BRENNEN, C. E. 1985*b* Chute flows of granular material: some computer simulations. *Trans. ASME* E: *J. Appl. Mech.* **52**, 172–178.

CARNAHAN, N. F. & STARLING, K. E. 1969 Equation of state for nonattracting rigid spheres. *J. Chem. Phys.* **51**, 635–636.

CHAPMAN, S. & COWLING, T. G. 1970 *The Mathematical Theory of Non-Uniform Gases*, 3rd edn. Cambridge University Press.

CUNDALL, P. A. 1974 A computer model for rock-mass behaviour using interactive graphics for input and output of geometrical data. US Army Corps. of Engrs (Missouri River Div.) *Tech. Rep. No.* MRD-2074.

HANES, D. M. 1983 Studies on the mechanics of rapidly flowing granular-fluid materials. Ph.D. thesis, University of California, San Diego.

HANES, D. M. & INMAN, D. L. 1985 Observations of rapidly flowing granular-fluid flow. *J. Fluid Mech.* **150**, 357–380.

JENKINS, J. T. & SAVAGE, S. B. 1983 A theory for the rapid flow of identical, smooth, nearly elastic particles. *J. Fluid Mech.* **130**, 187–202.

KANATANI, K. 1979*a* A micropolar continuum theory of granular materials. *Intl J. Engng Sci.* **17**, 419–432.

KANATANI, K. 1979*b* A continuum theory for the flow of granular materials. In *Theoretical and Applied Mechanics* (ed. Japan Natl Comm. for Theor. Appl. Mech.), vol. 27, pp. 571–578.

KANATANI, K. 1980 A continuum theory for the flow of granular materials (II). In *Theoretical and Applied Mechanics* (ed. Japan Natl Comm. for Theor. Appl. Mech.), vol. 28, pp. 485–497.

LUN, C. K. K. & SAVAGE, S. B. 1985 A simple kinetic theory for granular flow of rough, inelastic, spherical particles. *Trans. ASME* E: *J. Appl. Mech.* (to appear).

LUN, C. K. K., SAVAGE, S. B., JEFFREY, D. J. & CHEPURNIY, N. 1984 Kinetic theories for granular flow: inelastic particles in Couette flow and slightly inelastic particles in a general flowfield. *J. Fluid Mech.* **140**, 223–256.

MCTIGUE, D. F. 1978 A model for stresses in shear flows of granular material. In *Proc. US–Japan Sem. on Continuum-Mechanical and Statistical Approaches in the Mechanics of Granular Materials*, pp. 266–271.

MROZ, A. 1980 On hypoelasticity and plasticity approaches to constitutive modeling of the inelastic behaviour of soils. *Intl J. Numer. and Anal. Meth. in Geomech.* **4**, 45–55.

OGAWA, S. 1978 Multi-temperature theory of granular materials. In *Proc. US–Japan Sem. on Continuum-Mechanical and Statistical Approaches in the Mechanics of Granular Materials*, pp. 208–217.

OGAWA, S. & OSHIMA, N. 1977 A thermomechanical theory of soil-like materials. In *Theoretical and Applied Mechanics* (ed. Japan Natl Comm. for Theor. Appl. Mech.), vol. 25, pp. 229–244.

OSHIMA, N. 1978 Continuum model of fluidized granular media, In *Proc. U.S.–Japan Seminar on Continuum-Mechanical and Statistical Approaches in the Mechanics of Granular Materials*, pp. 189–202.

OSHIMA, N. 1980 Dynamics of fluidized granular material. In *Theoretical and Applied Mechanics* (ed. Japan Natl Comm. for Theor. Appl. Mech.), vol. 28, pp. 475–84.

SAVAGE, S. B. 1979 Gravity flow of cohesionless granular materials in chutes and channels. *J. Fluid Mech.* **92**, 53–96.

SAVAGE, S. B. 1984 The mechanics of rapid granular flows, *Advances in Applied Mechanics*, vol. 24 (ed. J. Hutchinson & T. Y. Wu), pp. 289–366. Academic.

SAVAGE, S. C. & JEFFREY, D. J. 1981 The stress tensor in a granular flow at high shear rates. *J. Fluid Mech.* **110**, 255–272.

SAVAGE, S. B. & SAYED, M. 1984 Stresses developed by dry cohesionless granular materials in an annular shear cell. *J. Fluid Mech.* **142**, 391–430.

SPENCER, A. J. M. 1981 Deformation of an ideal granular material. In *Mechanics of Solids, Rodney Hill 60 Anniversary Volume* (ed. H. G. Hopkins & J. J. Sewell), Pergamon.

WALTON, O. R. 1980 Particle dynamic modelling of geological materials. *Univ. of Ca. Lawrence Livermore Lab. Rep. UCRL*-52915.

WALTON, O. R. 1982*a* Explicit particle dynamics model for granular materials. *Univ. of Ca. Lawrence Livermore Lab., Rep. UCRL*-86260.

WALTON, O. R. 1982*b* Particle-dynamic calculations of shear flows. *Univ. of Ca. Lawrence Livermore Lab. Rep. UCRL*-88560.